Geomorphology 298 (2017) 63–71

Contents lists available at ScienceDirect

Geomorphology

journal homepage: www.elsevier.com/locate/geomorph

Terrestrial cosmogenic surface exposure dating of moraines at Lake Tahoe in the Sierra Nevada of California and slip rate estimate for the West Tahoe Fault

Ian K.D. Pierce [a,*], Steven G. Wesnousky [a], Lewis A. Owen [b]

[a] Center for Neotectonic Studies and Seismological Laboratory, University of Nevada, Reno, NV 89557, USA
[b] Department of Geology, University of Cincinnati, Cincinnati, OH 45221, USA

ARTICLE INFO

Article history:
Received 11 July 2017
Received in revised form 21 September 2017
Accepted 21 September 2017
Available online 27 September 2017

Keywords:
Sierra Nevada glaciation
Walker Lane
Slip rate
Cosmogenic exposure age

ABSTRACT

Two sets of Pleistocene moraines (Tioga and Tahoe) are preserved at Cascade Lake along the west side of Lake Tahoe. The ^{10}Be terrestrial cosmogenic nuclide surface exposure ages for two younger Tioga moraines yield an average age of 22.3 ± 1.2 ka, coincident with the global Last Glacial Maximum. The ages suggest that the Tioga glaciation may have reached its maximum several thousand years earlier in the Lake Tahoe basin than to the south along the east flank of the Sierra Nevada. The oldest ^{10}Be age (120 ± 8 ka) determined for an additional suite of 10 boulders exhibiting significant scatter in ^{10}Be ages is interpreted to be the minimum age of formation for older Tahoe moraines in the Tahoe basin, suggesting they were deposited during marine oxygen isotope stage 6. The moraines at Cascade Lake are displaced by the West Tahoe Fault that strikes northward for 45 km along the western edge of the Lake Tahoe basin. Vertical displacements of the crests of the Tahoe and Tioga moraines are 59 ± 10 and 32 ± 12 m respectively. Averaged over the time since the formation of the Tahoe and Tioga moraines, the average vertical separation rates are <0.5 ± 0.1 and ~1.4 ± 0.7 mm/y respectively. The measured vertical separation across the broad graben on the Tioga moraine may be accentuated by its deposition on a preexisting scarp and, in this regard, the increase in slip rate since the Tioga glaciation may be apparent rather than real. The fault slip rate and accompanying horizontal rate of extension averaged over the time since the formation of the older Tahoe moraines are respectively 0.6 ± 0.2 and 0.3 ± 0.2 mm/y. The slip rate averaged over the time since emplacement of the Tahoe moraine is in general accord with prior geologic studies reporting slip rate estimates elsewhere along the fault, and the horizontal extension rate is at the lower end of extension rates estimated by others with geodesy across the Tahoe basin.

1. Introduction

Two sets of Pleistocene moraines (Tioga and Tahoe) are preserved at Cascade Lake along the west side of Lake Tahoe (Figs. 1, 2). Each are displaced by the West Tahoe Fault, a normal fault that strikes ~45 km along the west side of the Tahoe basin. The Tahoe basin is largely the result of normal displacement across the West Tahoe Fault (Fig. 1). Here, we present 16 new and 4 recalculated terrestrial cosmogenic nuclide (TCN) exposure ages of boulders on the moraines to place limits on the timing of the Last Glacial Maximum (LGM) recorded by the Tioga moraine and the emplacement of the older Tahoe moraine at Cascade Lake. The estimated ages of the moraines are additionally used in conjunction with lidar measurements of the offsets across the moraines to estimate the West Tahoe Fault slip rate and extension rate across the basin. The resulting suite of observations and calculations provide new information that complements prior and similar studies of glacial history across the Sierra Nevada and geologic studies that have estimated the slip rate of the West Tahoe Fault.

2. Tectonic setting

The Lake Tahoe basin is a half-graben within the Walker Lane: a 500-km-long × 100-km-wide northwest-trending zone of discontinuous active faults and complex topography that accommodates up to 25% of the ~50 mm/y of dextral shear between the Pacific and North American plates (Thatcher et al., 1999; Dixon et al., 2000; Bennett et al., 2003; Unruh et al., 2003) (Fig. 3). The Walker Lane is located between the Sierra Nevada to the west and the north-northeast-trending normal faults of the Basin and Range to the east and is manifest geodetically as a zone of ~6–12 mm/y of northwest-directed right-lateral shear (e.g., Dixon et al., 2000; Hammond et al., 2011). The shear field is transtensional and accommodated by an array of northwest-striking

* Corresponding author.
E-mail address: ian@nevada.unr.edu (I.K.D. Pierce).

https://doi.org/10.1016/j.geomorph.2017.09.030
0169-555X/

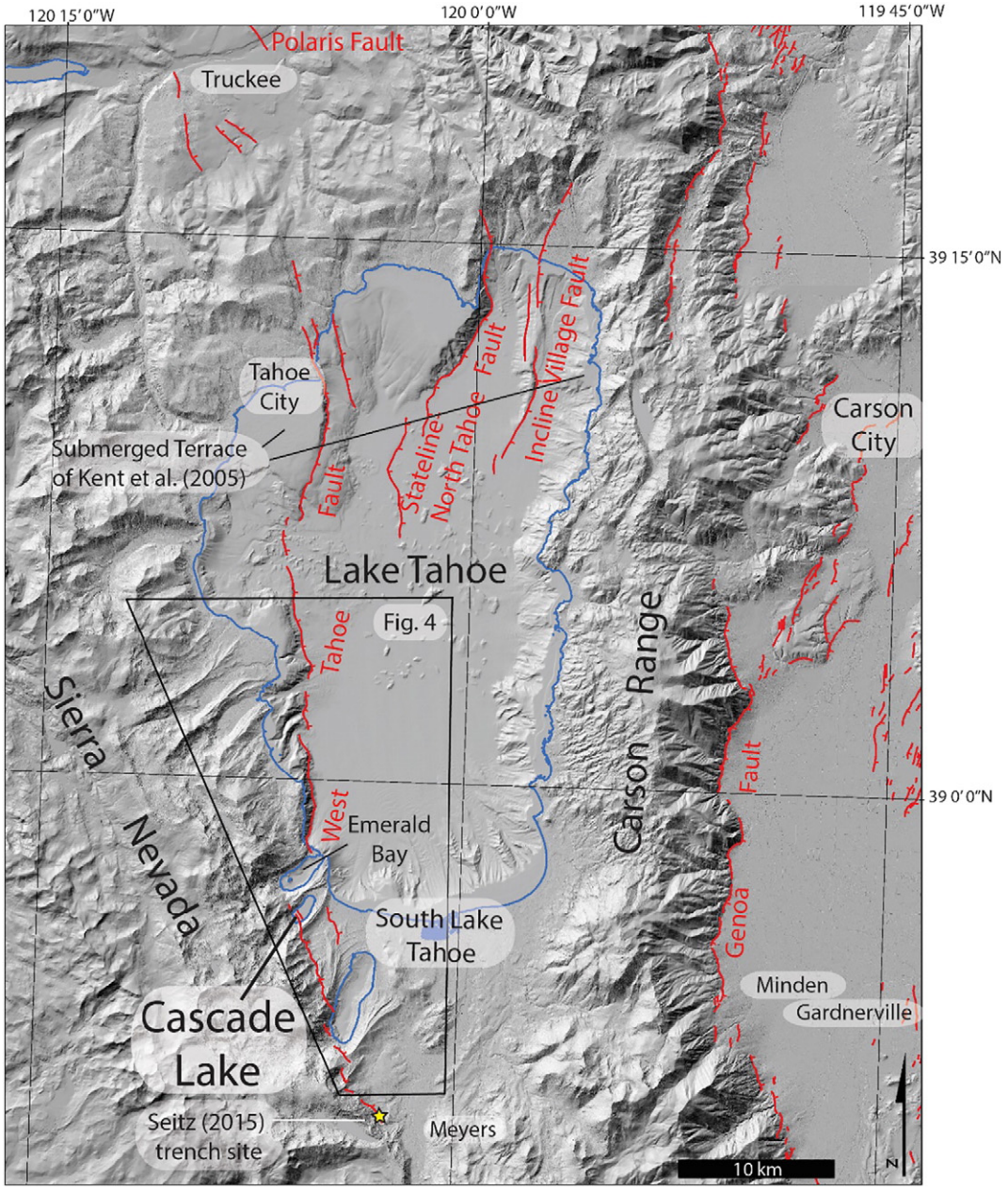

Fig. 1. Location of Lake Tahoe basin, the West Tahoe Fault, and surrounding area on hillshade image constructed from 10-m National Elevation Dataset topographic data and bathymetric data (Gardner et al., 2000). Contours of Lake Tahoe and Cascade Lake shorelines shown are blue. Active faults are in red and are modified after Kent et al. (2016) and the USGS Quaternary Fault and Fold Database (USGS, 2017). Kent et al. (2005) used the difference in elevation of submerged terraces to estimate a vertical separation rate of 0.5–0.75 mm/y across the basin. The location of Seitz (2015) trench site on the West Tahoe Fault is indicated with a star.

strike-slip faults, north-striking normal faults, and northeast striking left-lateral faults (e.g., Wesnousky, 2005). Within the vicinity of Lake Tahoe, northwest-striking strike-slip faults include the Polaris, Pyramid Lake, and Mohawk Valley faults; and the Olinghouse Fault is an example of a northwest-trending left-lateral fault (Fig. 3). The West Tahoe Fault is a prime example of a range-bounding normal fault in the region and shares strike direction with the nearby Genoa, Antelope Valley, and Smith Valley range-bounding normal faults as well as the largely subaqueous Stateline-North Tahoe and Incline Village faults within the Tahoe basin (Figs. 1, 3).

3. Framework of glacial history of region

The shoreline elevation of Lake Tahoe is ~1900 m above mean sea level (amsl), and the highest surrounding peaks of the Sierra Nevada and Carson Ranges reach in excess of 3000 m amsl (Fig. 1). Glacially carved U-shaped valleys and moraines are present along the western margin of the lake. Average annual precipitation at the lake is ~520 mm/y, occurs largely as snow, and increases westward with elevation to 1440 mm near the Sierra Nevada crest (NOAA, 2012).

Blackwelder (1931) was among the first to study glacial deposits throughout the Sierra Nevada and found two sets of moraines of distinctly different ages in most drainages of the Eastern Sierra (Fullerton, 1986; Gillespie and Clark, 2011). He and others since have attributed the moraines to two distinct late Pleistocene glacial stages and labeled the younger *Tioga* and the older *Tahoe* (e.g., Blackwelder, 1931; Putnam, 1949, 1960; Sharp and Birman, 1963; Birkeland, 1964; Birman, 1964; Clark, 1967; Sharp, 1972). They observed that the older Tahoe moraines are broader crested compared to younger Tioga

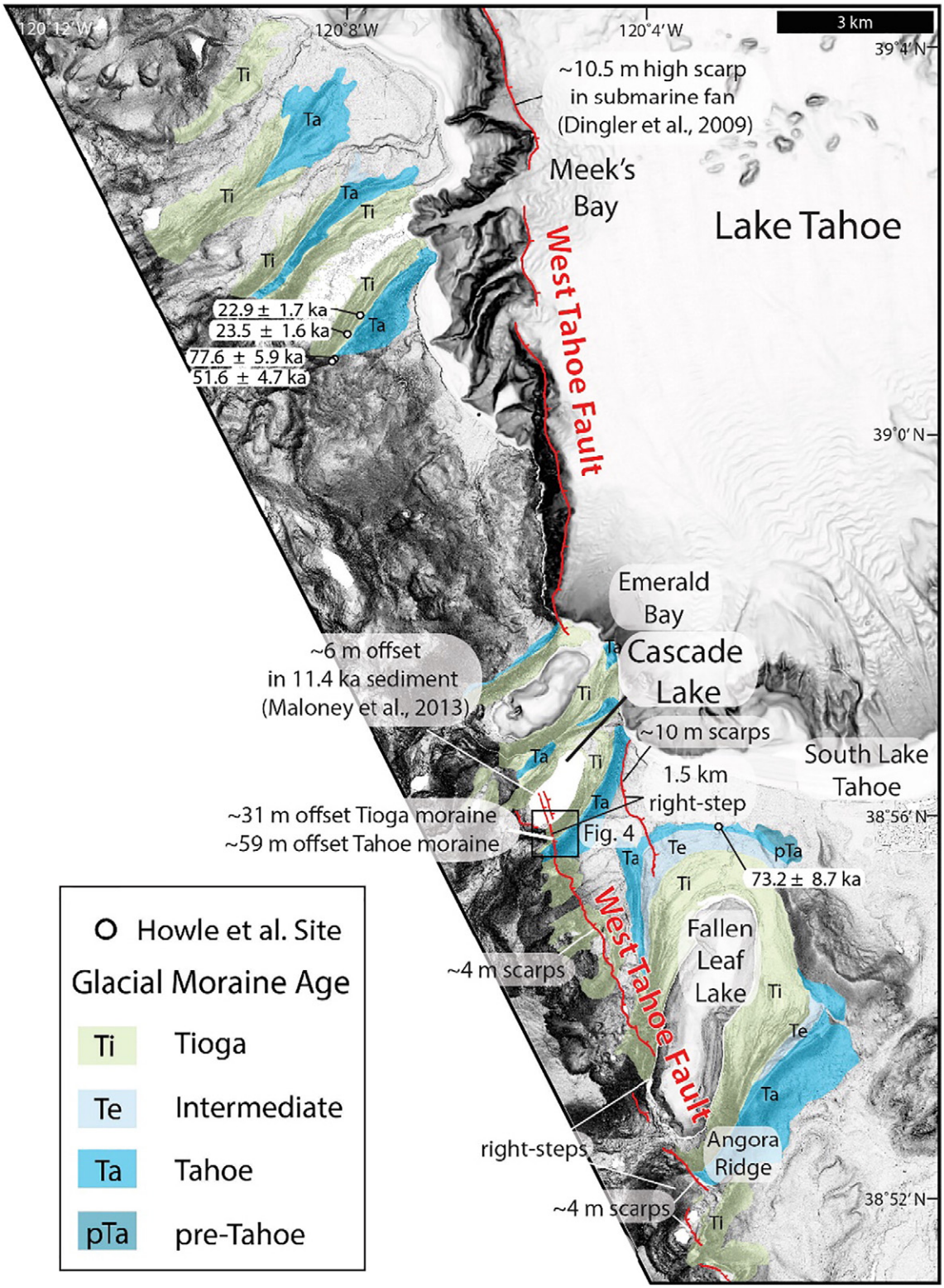

Fig. 2. Map of Tioga (green) and Tahoe age (blue) moraines along the southwest edge of the Tahoe basin. Trace of the West Tahoe Fault is red and displays right-step near Cascade Lake. Numerical ages on Meeks Bay moraines and Fallen Leaf Lake are discussed in text. Basemap is a hillshade constructed from 0.5-m lidar and 10-m bathymetric data (Gardner et al., 2000; Watershed Sciences, 2011).

moraines; that the granitic boulders composing the Tahoe moraines are in a greater state of disintegration than those on Tioga moraines; that the frequency and clast size of granitic boulders on these older Tahoe deposits are less, while the remaining boulders are more ragged; and that the soil developed on younger tills is an ashen gray while reddish in older deposits.

Researchers have more recently been able to determine numerical ages of moraines within the Sierra Nevada and elsewhere using TCN surface exposure dating techniques (e.g., Phillips et al., 1990; Gosse and Phillips, 2001). Rood et al. (2011a) undertook the broadest application of TCN analysis to glacial deposits in the Sierra Nevada examining moraines to the south of Lake Tahoe encompassing 12 canyons extending

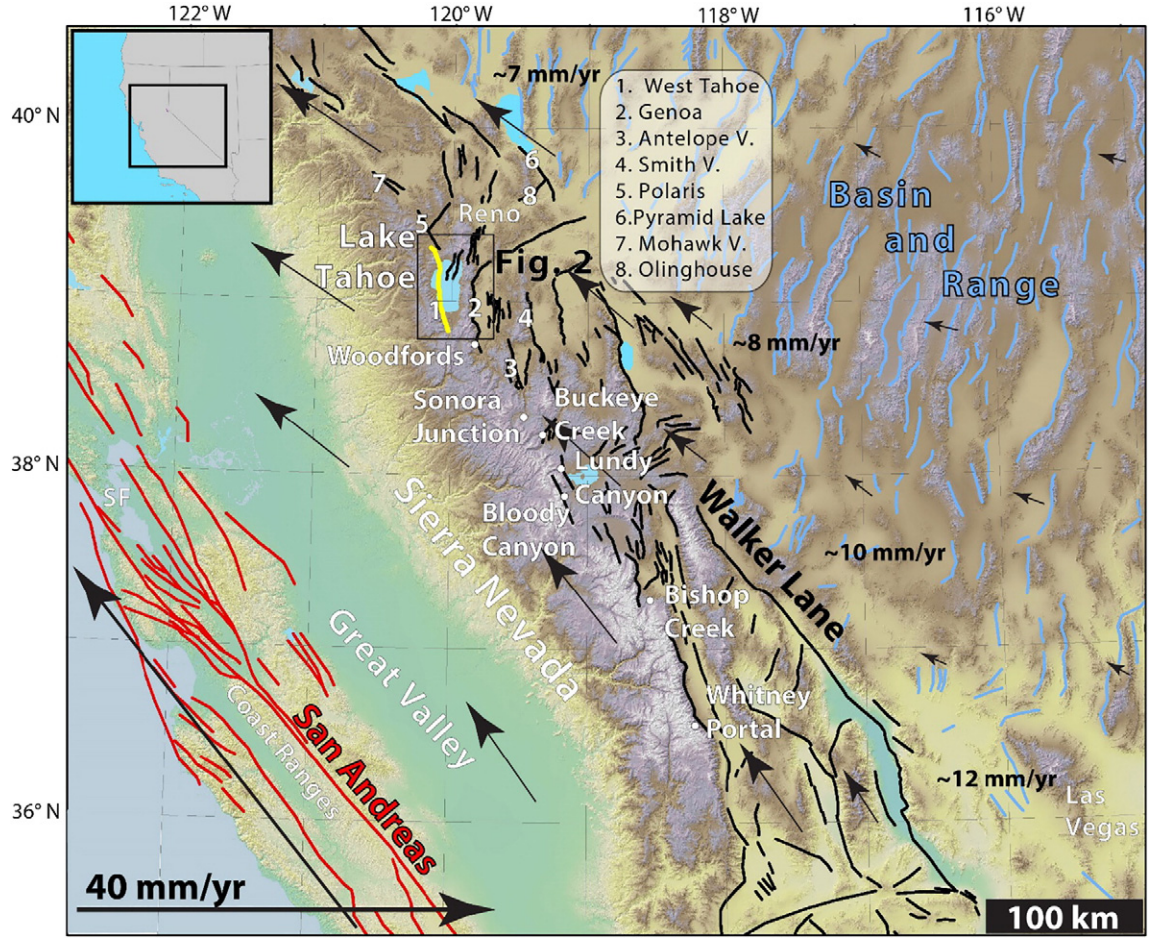

Fig. 3. Location of Lake Tahoe and West Tahoe Fault (yellow line) within Walker Lane. Faults of Walker Lane, the San Andreas Fault, and Basin and Range fault systems shown in black, red, and blue respectively. Faults and locations discussed in text are numbered and labeled. Black GPS vectors relative to a stable North America are modified after Flesch et al. (2000), and values in black refer to the approximate shear rate accommodated across the Walker Lane at their respective latitude after Hammond et al. (2011) and Dixon et al. (2000). Faults are simplified from the USGS Quaternary Fault and Fold Database (USGS, 2017).

from Whitney Portal to Woodfords along the eastern flank of the Sierra Nevada (Fig. 3). They conclude that major moraines of the eastern Sierra Nevada were deposited during marine isotope stages (MIS) 6 and 2, that retreat of each commenced at ~145 and ~18.8 ± 1.9 ka respectively, and that their observations and analyses provided no evidence for glacial advances intermediate to these ages. Rood et al. (2011a) followed convention and refered to the moraines and outwash of these deposits as Tahoe and Tioga for the older and younger major advances respectively. Phillips et al.'s (1990) TCN analysis of moraines at Bloody Canyon (Fig. 3) in contrast presents evidence for glacial advances intermediate in age to those identified as Tahoe and Tioga age by Rood et al. (2011a). Whether the absence of intermediate stage moraines in the canyons studied by Rood et al. (2011a) is caused by, e.g., obliterative overlap (Gibbons et al., 1984), sampling bias, or other unique conditions of moraine preservation at Bloody Canyon is unclear.

4. Data analysis and observations

4.1. TCN dating of moraines at Cascade Lake

Moraine ages are estimated here using measurements of TCN ^{10}Be concentrations in surface boulders. Sampling focused on the largest (>1 m in height) granitic boulders from each of the two right-lateral moraine crests at Cascade Lake with the intent to limit the possibility of post-depositional transportation or exhumation/denudation and to reduce the likelihood that the boulders were covered with snow for much of the year. Computational models of moraine erosion (e.g., Putkonen and Swanson, 2003) suggest that for old moraines (e.g., Tahoe), with a sufficient sample size of 6–7 boulders, it is likely (>90%) that the oldest measured age is close to the actual age of the deposit. In this study, we sampled 8 boulders on each moraine surface and treated the oldest age sampled as a minimum age of deposition. Four boulders each were sampled from the hanging and footwall surfaces of the Tioga and Tahoe moraines (Fig. 4). Approximately 500-g samples were taken from the upper 2–5 cm of each of these boulders. Photographs of each of the sampled boulders are provided in supplemental materials. All 16 samples were processed in the Geochronology Laboratories at the University of Cincinnati following the methods of Kohl and Nishiizumi (1992) and described in detail in supplemental materials. Additionally, ^{10}Be ages from two boulders from a Tioga moraine and two boulders from a Tahoe moraine near Meek's Bay (Fig. 2) — collected and processed by Howle et al. (2012) — are recalculated here and included in this analysis.

The TCN exposure ages are calculated using the Cosmic Ray Exposure Program (CREp) of Martin et al. (2017) and listed in Table 1. The ages reflect the increased concentrations of ^{10}Be that occur in rock as a function of the time they are exposed to cosmic rays at the Earth's surface. The calculator requires input describing the geographic coordinates and elevation of the samples, local shielding of the sample, density of the sample, and estimation of the boulder erosion rates resulting from processes such

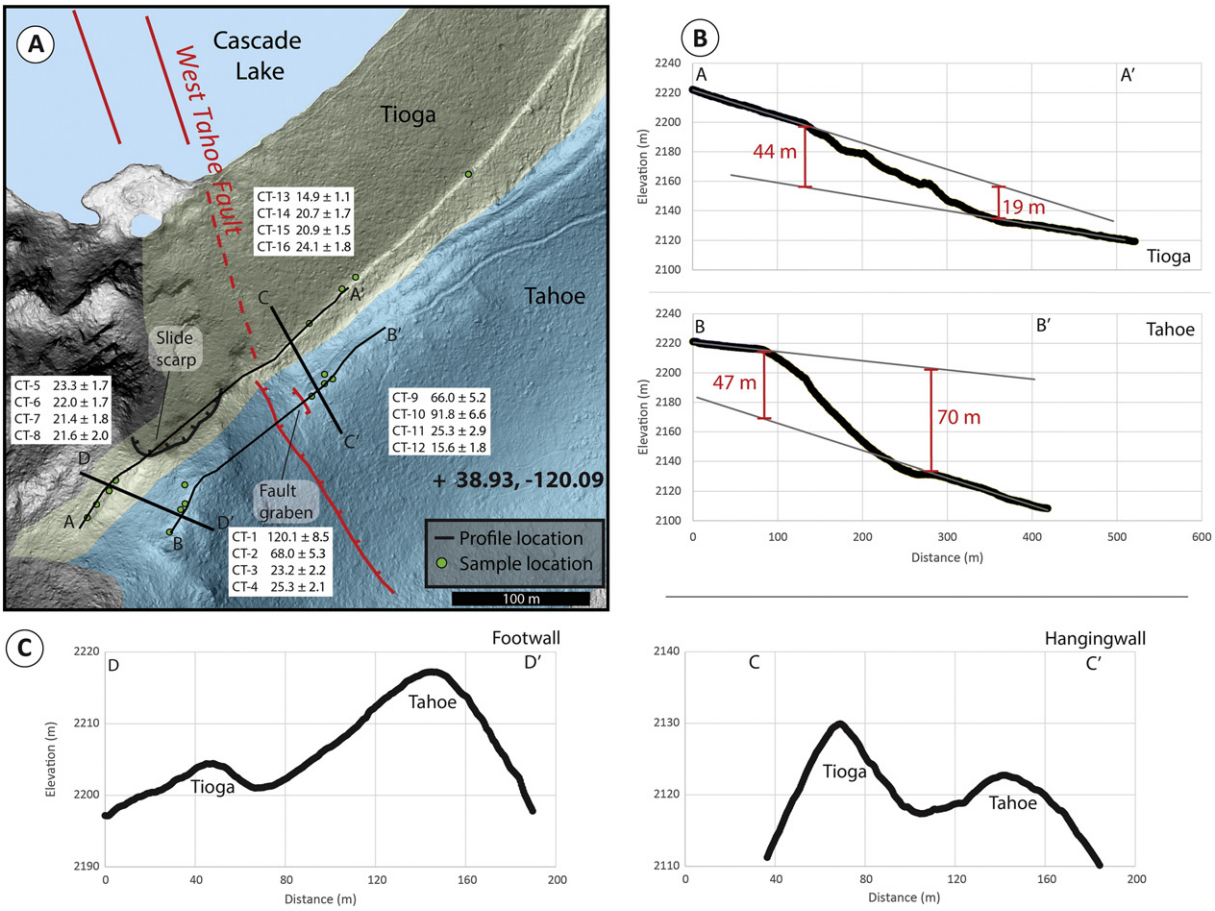

Fig. 4. (A) Locations, labels, and surface exposure ages (ka) of boulders sampled on Tioga (green) and Tahoe (blue) moraines at Cascade Lake. Locations of topographic profiles AA′ and BB′ along the moraine crests and CC′ and DD′ transverse to moraine crests are shown in (B) and (C) respectively. Geographic coordinate (+) provided for geographic reference.

as boulder grussification and spalling (Gosse and Phillips, 2001). These values are listed for each sample in Table 1. The calculations are made for convenience of later comparison using the same 0.6 m/Ma erosion rate employed by Rood et al. (2011a) in their study of numerous moraines along the eastern flank of the Sierra Nevada; and for reference, ages assuming bounding erosion rate values of zero and a maximum rate of 3.1 m/Ma based on erosion rates of bedrock summits in the Sierra Nevada (Small et al., 1997) are also provided. The age estimates are also dependent on the assumption of particular scaling models designed to estimate the long-term production rate of cosmogenic ^{10}Be. The ages in Table 1 use a production rate of 4.00 ± 0.3 atg^{-1} y^{-1} determined at Twin Lakes, which is located at a similar elevation to the moraines at Cascade Lake and ~12 km to the southwest (Nishiizumi et al., 1989; Balco et al., 2008; Borchers et al., 2016), the ERA40 atmosphere model of Uppala et al. (2005), the Lifton-VDM2016 geomagnetic database (Lifton, 2016), and the time-dependent scaling model of Lal (1991) and Stone (2000). For additional reference, we place in Table S1 of the supplemental materials the age estimates for each boulder using an alternate calculator (CRONUS v3.0; Balco et al., 2008) and a suite of alternate available production rate models (e.g., Lifton et al., 2014). Assumption of the various different production models yields changes in age estimates up to ±7% for a given assumed erosion rate (supplemental materials Table S1).

The exposure ages for each boulder calculated for the 0.6 m/Ma erosion rate and listed in Table 1 are presented graphically in Fig. 5. The data are divided according to the moraines on which the respective boulders were collected. The upper plots show age estimates (open circles) and 1σ error bars for the 0.6 m/Ma erosion rate. Values for bounding erosion rates of 0 and 3.1 m/Ma are also shown without error bars by asterisks and crosses respectively. The age estimates for 0.6 m/Ma erosion rate are further presented as individual probability density functions in the lower plots. The blue areas depict the sum of the individual probability density functions. The values and distributions of ages are addressed in the discussion section.

4.2. Displacement of Cascade moraines by West Tahoe Fault

The West Tahoe Fault strikes northerly ~45 km from near Meyers in the south to Tahoe City in the north (Fig. 1). The fault is largely subaqueous along its northern extent (Kent et al., 2005; Brothers et al., 2009; Dingler et al., 2009; Maloney et al., 2013) and steps ~1.5 km onshore near Emerald Bay where two strands of the fault cut the moraines at Cascade Lake (Fig. 2). The eastern of the two strands exhibits only an ~10-m-high fault scarp along the distal toe of the older Tahoe moraine. The western of the two strands, where it produces larger scarps in Tahoe and Tioga age moraines, is the focus of interest here. To assess the displacement where the fault cuts the moraine crests, topographic profiles are constructed along each of the Tioga and Tahoe moraine crests using ArcGIS v10.3 and the 0.5-m/pixel Lake Tahoe lidar DEM (Watershed Sciences, 2011). The profiles AA′ and BB′ and their locations are shown in Figs. 4A,B. The profiles illustrate that the breadth of the fault scarps exceed 100 m and that the slopes of the hanging and footwall surfaces do not match. Whether the mismatch in slopes reflects a component of tectonic deformation, original changes in slope of the

Table 1
Be-10 sample locations, concentrations and exposure ages.

Sample name	Latitude (°N)	Longitude (°W)	Altitude (m asl)	Sample thickness (cm)	^{10}Be concentration (10^3 atoms/g)	Minimum age[a] 0.0 m/Ma erosion (ka)	Preferred age[a] 0.6 m/Ma erosion (ka)	Maximum age[a] 3.1 m/Ma erosion (ka)
Tahoe Footwall								
CT-1	38.9298	120.0947	2221	2	2264 ± 40	113.0 ± 7.8	120.1 ± 8.5	180.2 ± 12.8
CT-2	38.9300	120.0946	2217	2	1297 ± 40	65.6 ± 4.9	68.0 ± 5.3	81.6 ± 6.5
CT-3	38.9303	120.0945	2213	2	452 ± 33	23.0 ± 2.2	23.2 ± 2.2	24.4 ± 2.4
CT-4	38.9301	120.0945	2217	2	495 ± 25	25.0 ± 2.1	25.3 ± 2.1	26.7 ± 2.3
Tioga Footwall								
CT-5	38.9300	120.0961	2218	2	454 ± 14	23.0 ± 1.7	23.3 ± 1.7	24.4 ± 1.8
CT-6	38.9301	120.0959	2214	2	427 ± 19	21.8 ± 1.7	22.0 ± 1.7	23.1 ± 1.8
CT-7	38.9306	120.0953	2209	2	411 ± 23	21.1 ± 1.7	21.4 ± 1.8	22.3 ± 1.9
CT-8	38.9304	120.0956	2206	2	416 ± 29	21.4 ± 1.9	21.6 ± 2.0	22.6 ± 2.1
Tahoe Hangingwall								
CT-9	38.9317	120.0922	2124	2	1183 ± 45	64.0 ± 4.9	66.0 ± 5.2	78.6 ± 6.5
CT-10	38.9316	120.0921	2134	2	1628 ± 33	87.6 ± 6.4	91.8 ± 6.6	116.7 ± 8.2
CT-11	38.9316	120.0922	2132	4	462 ± 45	25.0 ± 2.8	25.3 ± 2.9	26.8 ± 3.1
CT-12	38.9314	120.0924	2135	1	282 ± 29	15.5 ± 1.8	15.6 ± 1.8	16.1 ± 1.9
Tioga Hangingwall								
CT-13	38.9323	120.0924	2126	2	265 ± 9	14.8 ± 1.1	14.9 ± 1.1	15.4 ± 1.2
CT-14	38.9327	120.0919	2130	2	376 ± 22	20.5 ± .1.7	20.7 ± .1.7	21.5 ± .1.8
CT-15	38.9329	120.0916	2126	2	379 ± 13	20.7 ± 1.5	20.9 ± 1.5	21.7 ± 1.6
CT-16	38.9341	120.0898	2116	2.5	438 ± 15	23.8 ± 1.8	24.1 ± 1.8	25.3 ± 1.9
Meeks Creek (Howle et al., 2012)								
MC1	39.0144	120.1390	2178	5	944 ± 22	50.0 ± 4.6	51.6 ± 4.7	59.2 ± 4.2
MC2	39.0148	120.1385	2203	5	1420 ± 24	74.6 ± 5.7	77.6 ± 5.9	95.2 ± 6.6
MC3	39.0191	120.1351	2147	5	428 ± 6	23.2 ± 1.6	23.5 ± 1.6	24.7 ± 1.7
MC4	39.0222	120.1317	2115	5	407 ± 12	22.6 ± 1.6	22.9 ± 1.7	24.0 ± 1.8

No shielding correction was required. Uncertainties expressed as 1 σ.
[a] Ages calculated using the CREp using a local production rate, and the Lal (1991)/Stone (2000) time-dependent scaling model, density of 2.7 g/cm^3 and 07KNSTD.

moraine across the broad area of the scarps, or elements of both is not known. We place bounds on the vertical separation of surfaces produced by faulting by extrapolating the slopes of the foot and hanging wall across the scarp. The vertical separation of the extrapolated surfaces is assumed to place limits on the actual vertical separation. Vertical separation is observed to be between 19 and 44 m (31.5 ± 12.5 m) and between 47 and 70 m (58.5 ± 11.5 m) across the Tioga and Tahoe moraines respectively. With the assumption of a possible range of dips between 50° and 70°, the vertical separation values equate to values of fault slip across the Tioga and Tahoe moraines equal to 38.8 ± 18.6 m and 70.7 ± 20.7 m respectively. The progressively greater offset on the Tahoe moraine has resulted in an inversion of relative moraine heights on either side of the fault (Fig. 4C).

5. Discussion

5.1. Moraine dating

The observations we have collected are of consequence to discussions of glacial history and of tectonics of Lake Tahoe, the eastern Sierra, and the northern Walker Lane. The presentation of TCN exposure ages for boulders on the Cascade Lake moraines in Fig. 5 illustrates a distinctly greater scatter in ^{10}Be ages found on the older Tahoe moraine as compared to the Tioga moraine. The ^{10}Be exposure ages of boulders on the Tioga moraines group closely with an average value of 22.3 ± 1.2 ka when the single young outlier is ignored. The larger scatter in ^{10}Be TCN surface exposure ages for boulders collected on older moraines is common and has generally been attributed to forest fire spallation and to erosion of till matrix and exhumation of originally buried boulders that occurs with the relatively longer time since deposition (e.g., Heyman et al., 2011). In this regard, when such scatter is observed, it is general practice to assume the maximum boulder exposure age is most representative or a minimum estimate of the landform age (e.g., Phillips et al., 2009; Rood et al., 2011a). The maximum exposure age that we determine for boulders on the Tahoe moraine at Cascade Lake is 120.1 ± 8 ka. Following this logic, our estimates place the age of the Last Glacial Maximum Tioga advance at 22.3 ± 1.2 ka and that of the maximum advance of the Tahoe moraine at before 120.1 ± 8.3 ka. The latter age is in general accord with Rood et al.'s (2011a) assessment that retreat of the Tahoe advance commenced at ~144 ka over the entirety of the southern Sierra Nevada and is significantly older than the TCN ages of the two boulders on a Tahoe moraine reported at nearby Meeks Bay (Fig. 2) — reported and interpreted by Howle et al. (2012) to indicate that Tahoe moraines correspond to MIS 4 of the oxygen-isotope record rather than MIS 6.

The 22.3 ± 1.2 ka age of the Tioga advance we obtain at Cascade Lake is older than the 18.8 ± 1.9 ka age determined by Rood et al. (2011a) for moraines attributed to the LGM in seven canyons ranging from ~60 to 240 km south of Lake Tahoe along the east flank of the Sierra Nevada (Fig. 3). Geographic differences that might contribute to the difference are the northern latitude of Lake Tahoe, the lower elevations at the crest of the northern Sierra compared to the central Sierra, the location of the Cascade Lake moraines adjacent to a major water source, and the higher rainfall that is characteristic of the Lake Tahoe region as compared to the sites studied by Rood et al. (2011a) along the eastern Sierran flank (NOAA, 2012), though exactly how these factors might affect this difference in timing is not clear.

5.2. Rates of faulting

The rate of vertical displacement occurring across the West Tahoe Fault at Cascade Lake is obtained here by respectively dividing the vertical separations of the Tioga (31.5 ± 12.5 m) and Tahoe (62 ± 15 m) moraines measured across the West Tahoe Fault (Fig. 4) by the estimated ages of the Tioga (22.3 ± 1.2 ka) and Tahoe (>120.1 ± 8.3 ka) moraines (Fig. 5). The exercise indicates that the vertical displacement averaged over >120.1 ± 8.3 ka has averaged no >0.5 ± 0.1 mm/y, and a faster vertical rate of 1.4 ± 0.7 mm/y when averaged over the last 22.3 ± 1.2 ka. If the additional ~10-m-high scarp in the toe of the

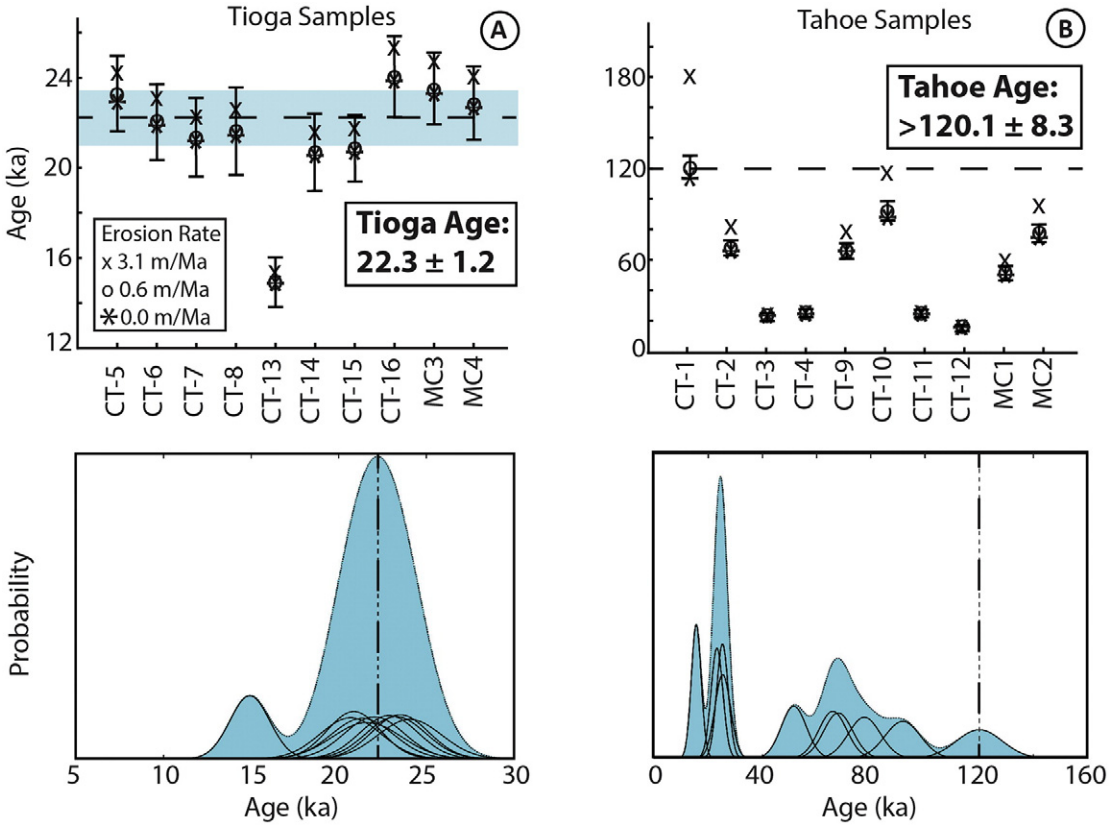

Fig. 5. Surface exposure ages of boulders on the (A) Tioga and (B) Tahoe moraines at Cascade Lake (CT) and Meek's Creek (MC). The upper plots show age estimates (open circles) and 1σ error bars for the 0.6 m/Ma erosion rate. Values for bounding erosion rates of 0 and 3.1 m/Ma are also shown without error bars by asterisks and crosses, respectively. The age estimates for 0.6 m/Ma erosion rate are presented as individual probability density functions in the lower plots. The blue areas depict the sum of the individual probability density functions. The ages and manner of calculation are listed in Table 1 and discussed in text.

Tahoe moraine on the eastern strand near Cascade Lake is added to the scarp in Fig. 4, the total vertical displacement rate increases to 0.6 ± 0.1 mm/y. Assuming that the vertical separations are the result of slip on a fault dipping between 50° and 70°, the corresponding post-Tioga and -Tahoe fault down-dip slip rates are $1.6\ ^{+1.1}_{-0.7}$ mm/y and 0.6 ± 0.2 mm/y, respectively. The results taken at face value suggest an increase in fault slip rate in post-Tioga time. We hesitate to argue strongly for the veracity of the rate increase because there are a number of reasons to suggest that the rate increase is apparent and not real. For example, such an increase is not observed in the numerous calculations of slip rate from the offset of Tioga and Tahoe moraines nearby and to the south (Rood et al., 2011b). Similarly, the post-Tioga rate that we calculate at Cascade Lake is significantly greater than those posited from displaced Tioga moraines along the Sierran frontal fault to the south of Lake Tahoe (Rood et al., 2011b) and nearby estimates of slip rate across the West Tahoe Fault, which include the 0.4–0.8 mm/y down-dip slip rate that Dingler et al. (2009) estimated from an ~10.5-m displacement of an assumed Tioga-aged submerged fan delta and a 0.5-mm/y vertical rate that can be calculated based on the ~6 m of offset observed in ~11.4-ka-old sediments in Cascade Lake by Maloney et al. (2013) (Fig. 2). Finally, because of the broad nature of the scarps at Cascade Lake and their location at a canyon mouth where gradients change rapidly caused by preceding fault displacements and scarp creation, a significant portion of the offset measured across what we define as the younger Tioga scarp may incorporate earlier pre-Tioga displacement. Alternately, if the rate increase is in fact real, one might speculate that it reflects a post-glacial increase in slip rate such as has been suggested in studies of faults along the Wasatch range of Utah (Hetzel and Hampel, 2005) and the Teton range in Wyoming (Hampel et al., 2007).

Our observations further confirm the displacement of the West Tahoe Fault in the late Pleistocene (Kent et al., 2005; Dingler et al., 2009; Howle et al., 2012; Maloney et al., 2013; Seitz, 2015; Kent et al., 2016). Yet, while geodesy shows that ~8 mm/y of northwest-directed right-lateral shear is accommodated across the northern Walker Lane, and specifically that in excess of ~1 mm of that right-lateral shear is accommodated across the Lake Tahoe basin (e.g., Hammond et al., 2011; Bormann et al., 2016), our observations of the West Tahoe Fault do not show evidence for a component of right-lateral strike-slip. Over Tioga and Tahoe timescales, if the West Tahoe Fault were accommodating this geodetically observed ~1 mm/y of right-lateral strike-slip, we would expect to see ~22 and ~120 m of right-lateral offset of the Tioga and Tahoe moraines at Cascade Lake respectively. The lack of evidence for strike-slip faulting remains an ongoing problem in the northern Walker Lane where the understanding of how dextral shear is accommodated in the absence of major thoroughgoing strike-slip faults remains poorly understood (e.g., Wesnousky et al., 2012).

Seitz's (2015) excavations across the West Tahoe Fault a few kilometers south of Cascade Lake (Fig. 1) revealed evidence of three earthquakes during the last ~10 ka with average coseismic vertical displacements of ~1.1 m and suggesting an average return time of about 3.3 ka. Dividing the average coseismic vertical displacement of 1.1 m by our calculated post-Tahoe slip rate (0.6 ± 0.2 mm/y) at Cascade Lake results in an estimated repeat time of about 2.2 ka, generally consistent with the results of Seitz (2015). Were we to use the higher post-Tioga vertical rate of 1.4 ± 0.5 mm/y, the estimated return time would be ~800 years, significantly less and inconsistent with the return time suggested by observations undertaken by Seitz (2015). Such inferences need to be tempered by the fact that earthquake recurrence is variable and not periodic. For further

context, were the entirety of the 45-km-long West Tahoe Fault to rupture, empirical scaling laws predict that it would produce average vertical displacements of about 1.3 m (e.g., Wesnousky, 2008) with a moment-magnitude of 6.9 (Wells and Coppersmith, 1994).

6. Conclusion

Interpretation of ^{10}Be TCN surface exposure ages for boulders on moraines mapped as Tioga and Tahoe in relative age at Cascade Lake indicates that they were deposited at 22.3 ± 1.2 ka (1σ) and >120.1 ± 8.3 ka which is consistent with their emplacement during the LGM in MIS 2 and MIS 6 respectively. The results hint that recession of Tioga moraines commenced earlier, and analogously LGM occurred earlier, at the latitude of Lake Tahoe as compared to farther south in the Sierra Nevada. The offset of moraines at Cascade Lake when combined with the estimated moraine ages yield estimates of vertical separation rate across the West Tahoe Fault of 1.4 ± 0.7 mm/y and 0.5 ± 0.1 mm/y since emplacement of the Tioga and Tahoe moraines respectively. The increase in slip rate since Tioga time is viewed to more likely be apparent than real. The slip rate when averaged over time since emplacement of the Tahoe moraine is consistent with geologic reports of slip rate reported elsewhere along the fault system. The accompanying horizontal extension rate is at the lower end of values based on geodesy, as is common across many of the basins of the northern Walker Lane.

Acknowledgements

This research was supported in part by National Science Foundation grant EAR-1419724 and EAR-1419789 and by USGS grant G15AP00088. This paper was improved by a thoughtful review by Dr. I. S. Evans and editing by Dr. Richard A. Marston. We are truly grateful to Sarah Hammer and Steve Angster for help in processing samples in the lab, Graham Kent for his assistance in the field and discussions, Ken Adams for enlightening discussions, and the 2015 University of Nevada, Reno neotectonics class assistance in sampling. Any use of trade, firm, or product names is for descriptive purposes only and does not imply endorsement. Center for Neotectonics Studies Contribution No. 74.

Appendix A. Supplementary data

Supplementary data to this article can be found online at https://doi.org/10.1016/j.geomorph.2017.09.030.

References

Balco, G., Stone, J.O., Lifton, N.A., Dunai, T.J., 2008. A complete and easily accessible means of calculating surface exposure ages or erosion rates from ^{10}Be and ^{26}Al measurements. Quat. Geochronol. 3:174–195. https://doi.org/10.1016/j.quageo.2007.12.001.

Bennett, R.A., Wernicke, B.P., Niemi, N.A., Friedrich, A.M., Davis, J.L., 2003. Contemporary strain rates in the northern Basin and Range province from GPS data. Tectonics 22 (31 pp.). https://doi.org/10.1029/2001TC001355.

Birkeland, P.W., 1964. Pleistocene glaciation of the Northern Sierra Nevada, North of Lake Tahoe, California. J. Geol. 72, 810–825.

Birman, J.H., 1964. Glacial geology across the crest of the Sierra Nevada, California. Geol. Soc. Am. Spec. Pap. 75 (80 pp.).

Blackwelder, E., 1931. Pleistocene glaciation in the Sierra Nevada and basin ranges. Geol. Soc. Am. Bull. 42, 865–922.

Borchers, B., Marrero, S., Balco, G., Caffee, M., Goehring, B., Lifton, N., Nishiizumi, K., Phillips, F., Schaefer, J., Stone, J., 2016. Geological calibration of spallation production rates in the CRONUS-Earth project. Quat. Geochronol. 31:188–198. https://doi.org/10.1016/j.quageo.2015.01.009.

Bormann, J.M., Hammond, W.C., Kreemer, C., Blewitt, G., 2016. Accommodation of missing shear strain in the Central Walker Lane, western North America: Constraints from dense GPS measurements. Earth Planet. Sci. Lett. 440:169–177. https://doi.org/10.1016/j.epsl.2016.01.015.

Brothers, D.S., Kent, G.M., Driscoll, N.W., Smith, S.B., Karlin, R., Dingler, J.A., Harding, A.J., Seitz, G.G., Babcock, J.M., 2009. New constraints on deformation, slip rate, and timing of the most recent earthquake on the West Tahoe-Dollar Point Fault, Lake Tahoe Basin, California. Bull. Seismol. Soc. Am. 99:499–519. https://doi.org/10.1785/0120080135.

Clark, M.M., 1967. Pleistocene glaciation of the upper West Walker drainage, Sierra Nevada, California (Dissertation). Stanford University, Stanford.

Dingler, J., Kent, G., Babcock, J., Harding, A., Seitz, G., Karlin, B., Goldman, C., 2009. A high-resolution seismic CHIRP investigation of active normal faulting across Lake Tahoe Basin, California-Nevada. GSA Bull. 121, 1089–1107.

Dixon, T.H., Miller, M., Farina, F., Wang, H., Johnson, D., 2000. Present-day motion of the Sierra Nevada block and some tectonic implications for the Basin and Range province, North American Cordillera. Tectonics 19, 1–24.

Flesch, L.M., Holt, W.E., Haines, A.J., Shen-Tu, B., 2000. Dynamics of the Pacific-North American plate boundary in the western United States. Science 287, 834–836.

Fullerton, D.S., 1986. Chronology and correlation of glacial deposits in the Sierra Nevada, California. Quat. Sci. Rev. 5, 161–169.

Gardner, J.V., Mayer, L.A., Clarke, J.E.H., 2000. Morphology and processes in Lake Tahoe (California-Nevada). Geol. Soc. Am. Bull. 112, 736–746.

Gibbons, A.B., Megeath, J.D., Pierce, K.L., 1984. Probability of moraine survival in a succession of glacial advances. Geology 12, 327–330.

Gillespie, A.R., Clark, D.H., 2011. Glaciations of the Sierra Nevada, California, USA. Developments in Quaternary Sciences. Elsevier, pp. 447–462.

Gosse, J.C., Phillips, F.M., 2001. Terrestrial in situ cosmogenic nuclides: theory and application. Quat. Sci. Rev. 20, 1475–1560.

Hammond, W.C., Blewitt, G., Kreemer, C., 2011. Block modeling of crustal deformation of the northern Walker Lane and Basin and Range from GPS velocities. J. Geophys. Res. 116. https://doi.org/10.1029/2010JB007817.

Hampel, A., Hetzel, R., Densmore, A.L., 2007. Postglacial slip-rate increase on the Teton normal fault, northern Basin and Range Province, caused by melting of the Yellowstone ice cap and deglaciation of the Teton Range? Geology 35, 1107–1110.

Hetzel, R., Hampel, A., 2005. Slip rate variations on normal faults during glacial-interglacial changes in surface loads. Nature 435, 81–84.

Heyman, J., Stroeven, A.P., Harbor, J.M., Caffee, M.W., 2011. Too young or too old: evaluating cosmogenic exposure dating based on an analysis of compiled boulder exposure ages. Earth Planet. Sci. Lett. 302:71–80. https://doi.org/10.1016/j.epsl.2010.11.040.

Howle, J.F., Bawden, G.W., Schweickert, R.A., Finkel, R.C., Hunter, L.E., Rose, R.S., von Twistern, B., 2012. Airborne LiDAR analysis and geochronology of faulted glacial moraines in the Tahoe-Sierra frontal fault zone reveal substantial seismic hazards in the Lake Tahoe region, California-Nevada, USA. Geol. Soc. Am. Bull. 124, 1087–1101.

Kent, G.M., Babcock, J.M., Driscoll, N.W., Harding, A.J., Dingler, J.A., Seitz, G.G., Gardner, J.V., Mayer, L.A., Goldman, C.R., Heyvaert, A.C., Richards, R.C., Karlin, R., Morgan, C.W., Gayes, P.T., Owen, L.A., 2005. 60 k.y. record of extension across the western boundary of the Basin and Range province: Estimate of slip rates from offset shoreline terraces and a catastrophic slide beneath Lake Tahoe. Geology 33:365–368. https://doi.org/10.1130/G21230.1.

Kent, G., Schmauder, G., Maloney, J., Driscoll, N., Kell, A., Smith, K., Baskin, R., Seitz, G., 2016. Reevaluating Late-Pleistocene and Holocene active faults in the Tahoe Basin, California-Nevada. Applied Geology in California, Special Publication. Associate of Environmental & Engineering Geologists, pp. 833–858.

Kohl, C.P., Nishiizumi, K., 1992. Chemical isolation of quartz for measurement of in-situ-produced cosmogenic nuclides. Geochim. Cosmochim. Acta 56, 3583–3587.

Lal, D., 1991. Cosmic ray labeling of erosion surfaces: in situ nuclide production rates and erosion models. Earth Planet. Sci. Lett. 104, 424–439.

Lifton, N., 2016. Implications of two Holocene time-dependent geomagnetic models for cosmogenic nuclide production rate scaling. Earth Planet. Sci. Lett. 433:257–268. https://doi.org/10.1016/j.epsl.2015.11.006.

Lifton, N., Sato, T., Dunai, T.J., 2014. Scaling in situ cosmogenic nuclide production rates using analytical approximations to atmospheric cosmic-ray fluxes. Earth Planet. Sci. Lett. 386:149–160. https://doi.org/10.1016/j.epsl.2013.10.052.

Maloney, J.M., Noble, P.J., Driscoll, N.W., Kent, G.M., Smith, S.B., Schmauder, G.C., Babcock, J.M., Baskin, R.L., Karlin, R., Kell, A.M., Seitz, G.G., Zimmerman, S., Kleppe, J.A., 2013. Paleoseismic history of the Fallen Leaf segment of the West Tahoe-Dollar Point fault reconstructed from slide deposits in the Lake Tahoe Basin, California-Nevada. Geosphere 9:1065–1090. https://doi.org/10.1130/GES00877.1.

Martin, L.C.P., Blard, P.-H., Balco, G., Lavé, J., Delunel, R., Lifton, N., Laurent, V., 2017. The CREp program and the ICE-D production rate calibration database: a fully parameterizable and updated online tool to compute cosmic-ray exposure ages. Quat. Geochronol. 38:25–49. https://doi.org/10.1016/j.quageo.2016.11.006.

Nishiizumi, K., Winterer, E.L., Kohl, C.P., Klein, J., Middleton, R., Lal, D., Arnold, J.R., 1989. Cosmic ray production rates of ^{10}Be and ^{26}Al in quartz from glacially polished rocks. J. Geophys. Res. Solid Earth 94:17907–17915. https://doi.org/10.1029/JB094iB12p17907.

NOAA, 2012. 1981–2010 Climate Normals.

Phillips, F.M., Zreda, M.G., Smith, S.S., Elmore, D., Kubik, P.W., Sharma, P., 1990. Cosmogenic chlorine-36 chronology for glacial deposits at Bloody Canyon, Eastern Sierra Nevada. Science 248, 1529–1532.

Phillips, F.M., Zreda, M., Plummer, M.A., Elmore, D., Clark, D.H., 2009. Glacial geology and chronology of Bishop Creek and vicinity, Eastern Sierra Nevada, California. Geol. Soc. Am. Bull. 121:1013–1033. https://doi.org/10.1130/B26271.1.

Putkonen, J., Swanson, T., 2003. Accuracy of cosmogenic ages for moraines. Quat. Res. 59: 255–261. https://doi.org/10.1016/S0033-5894(03)00006-1.

Putnam, W.C., 1949. Quaternary geology of the June Lake district, California. Geol. Soc. Am. Bull. 60, 1281–1302.

Putnam, W.C., 1960. Faulting and Pleistocene glaciation in the east-central Sierra Nevada of California, U.S.A. Nord. Intern. Geol Cong 21st Sess, pp. 270–274.

Rood, D.H., Burbank, D.W., Finkel, R.C., 2011a. Chronology of glaciations in the Sierra Nevada, California, from ^{10}Be surface exposure dating. Quat. Sci. Rev. 30:646–661. https://doi.org/10.1016/j.quascirev.2010.12.001.

Rood, D.H., Burbank, D.W., Finkel, R.C., 2011b. Spatiotemporal patterns of fault slip rates across the Central Sierra Nevada frontal fault zone. Earth Planet. Sci. Lett. 301: 457–468. https://doi.org/10.1016/j.epsl.2010.11.006.

Watershed Sciences, 2011. Lidar Remote Sensing Lake Tahoe Watershed, California/Nevada.
Seitz, G., 2015. The West Tahoe Fault (Fault Evaluation Report No. FER 261). California Geological Survey, Emerald Bay and Echo Lake Quadrangles, El Dorado County, California.
Sharp, R.P., 1972. Pleistocene glaciation, Bridgeport Basin, California. Geol. Soc. Am. Bull. 83, 2233–2260.
Sharp, R.P., Birman, J.H., 1963. Additions to classical sequence of Pleistocene glaciations, Sierra Nevada, California. Geol. Soc. Am. Bull. 74, 1079–1086.
Small, E.E., Anderson, R.S., Repka, J.L., Finkel, R., 1997. Erosion rates of alpine bedrock summit surfaces deduced from in situ ^{10}Be and ^{26}Al. Earth Planet. Sci. Lett. 150:413–425. https://doi.org/10.1016/S0012-821X(97)00092-7.
Stone, J.O., 2000. Air pressure and cosmogenic isotope production. J. Geophys. Res. 105, 23,753–23,759.
Thatcher, W., Foulger, G.R., Julian, B.R., Svarc, J., Quilty, E., Bawden, G.W., 1999. Present-day deformation across the Basin and Range Province, Western United States. Science 283, 1714–1717.
Unruh, J., Humphrey, J., Barron, A., 2003. Transtensional model for the Sierra Nevada frontal fault system, eastern California. Geology 31, 327–330.
Uppala, S.M., KAllberg, P.W., Simmons, A.J., Andrae, U., Bechtold, V.D.C., Fiorino, M., Gibson, J.K., Haseler, J., Hernandez, A., Kelly, G.A., Li, X., Onogi, K., Saarinen, S., Sokka, N., Allan, R.P., Andersson, E., Arpe, K., Balmaseda, M.A., Beljaars, A.C.M., Berg, L.V.D., Bidlot, J., Bormann, N., Caires, S., Chevallier, F., Dethof, A., Dragosavac, M., Fisher, M., Fuentes, M., Hagemann, S., Hólm, E., Hoskins, B.J., Isaksen, L., Janssen, P.A.E.M., Jenne, R., Mcnally, A.P., Mahfouf, J.-F., Morcrette, J.-J., Rayner, N.A., Saunders, R.W., Simon, P., Sterl, A., Trenberth, K.E., Untch, A., Vasiljevic, D., Viterbo, P., Woollen, J., 2005. The ERA-40 re-analysis. Q. J. R. Meteorol. Soc. 131:2961–3012. https://doi.org/10.1256/qj.04.176.
USGS, 2017. Quaternary Fault and Fold Database of the United States.
Wells, D.L., Coppersmith, K.J., 1994. New empirical relationships among magnitude, rupture length, rupture width, rupture area, and surface displacement. Bull. Seismol. Soc. Am. 84, 974–1002.
Wesnousky, S.G., 2005. Active faulting in the Walker Lane. Tectonics 24 (35 pp.). https://doi.org/10.1029/2004TC001645.
Wesnousky, S.G., 2008. Displacement and geometrical characteristics of earthquake surface ruptures: issues and implications for seismic-hazard analysis and the process of earthquake rupture. Bull. Seismol. Soc. Am. 98:1609–1632. https://doi.org/10.1785/0120070111.
Wesnousky, S.G., Bormann, J.M., Kreemer, C., Hammond, W.C., Brune, J.N., 2012. Neotectonics, geodesy, and seismic hazard in the Northern Walker Lane of Western North America: thirty kilometers of crustal shear and no strike-slip? Earth Planet. Sci. Lett. 329–330:133–140. https://doi.org/10.1016/j.epsl.2012.02.018.